Proc Indian Natn Sci Acad **80** No. 5 December 2014 pp. 941-948

DOI: 10.16943/ptinsa/2014/v80i5/47968

Review Article

Electron Spin Resonance Study of E_1' in Natural and γ-Ray-Irradiated Amethyst

G SIVARAMAIAH
Department of Physics, Government College for Men (A), Cuddapah 516004, India

(Received on 17 November 2013; Revised on 08 June 2014; Accepted on 29 October 2014)

The thermal properties such as Gibbs free energy, activation energy, entropy and enthalpy have been evaluated from the absolute number of spins of E_1' in gamma-ray-irradiated and as-is amethysts. It is for the first time to calculate the above properties for E_1' in amethyst. The Gibbs free energy of E_1' increases with the decrease of temperature from 296 K to 90 K. The activation energy and pre-exponential coefficients of E_1' have been evaluated from the logarithmic number of spins and the reciprocal of temperature plot. The Curie temperature and Curie constant of E_1' have been evaluated from the reciprocal of magnetic susceptibility and temperature plot. The exchange field, exchange integral and exchange interaction energy have been evaluated from the Curie temperature.

Key Words: ESR; E_1'; Gibbs Free Energy; Activation Energy; Entropy; Enthalpy

Introduction

E' paramagnetic defect centers are one of the best known families of charge defects found in quartz and silicate minerals (Weeks, 1956). Their main characteristic property is an unpaired electron trapped in or nearby an oxygen vacancy of the SiO_2 lattice. Several kinds of E' centers have been identified by means of Electron Spin Resonance (ESR) spectroscopy, besides E_1', E_2'and E_4' paramagnetic centers (Rudra *et al.*, 1985; Weeks and Nelson, 1960). In the 50 years since, the publication of the first paper on the Electron Paramagnetic Resonance (EPR) spectrum of the E' center, more than 3000 papers have been published in which the E' center is the important topic or an important sub-topic. More than 15 types of E' centers have been submitted in the past 50 years, new work continues. Agnello *et al.* (2002) have suggested that there are two structures for the E' center and a new variety of E' center was reported in 2006. The E' center concentration in natural crystals and silica is used to measure the age of geological specimens (Weeks *et al.*, 2008).

The E' paramagnetic defect center is a hole trap with the unpaired electron facing a $+Si{\equiv}O_3$ moiety. That assignment did fit in naturally with the theoretically calculated E_1' model (Weeks *et al.*, 2008) depicting the defect in crystalline a quartz as the $O_3{\equiv}Si.+Si{\equiv}O_3$ unit when in the paramagnetic state. The E' precursor is seen as a diamagnetic $O_3{\equiv}SiH$ paramagnetic center which upon hole trapping releases a mobile proton leading to the formation of a paramagnetic $O_3{\equiv}Si{\equiv}E'$ defect, as detected by ESR. The $O_3{\equiv}SiH$ precursors can operate as important for subsequent potential positive charging as a result of some external influence. Naturally, the presence of E' centers is taken as a measure of oxide quality.

Quartz (SiO_2) is one of the most abundant minerals in the earth's crust, and is a common component of archaeological artifacts and geological materials, being included in many rocks and sediments. It is present as an important mineral in meteorites and lunar and martian rocks (Wang *et al.*, 1998). The physical properties of natural quartz have found many applications in research areas, ranging

**Author for Correspondence: E-mail: gsivaram7@yahoo.co.in; Phone, +91 8562 244422*

from luminescence dating and radiation dosimetry to commercial areas such as gemology (Santos *et al.*, 2001; Schilles *et al*., 2001; Rocha *et al*., 2003; Sawakuchi and Okuno 2004). The most common polymorph is trigonal alpha-quartz which is composed exclusively of $[SiO_4]^{4-}$ tetrahedra with all oxygen atoms joined together in a three dimensional network. Substitution of silicon atoms in the lattice is rare because of the small ionic radius of Si^{4+} (0.42 °A) and the high valence. Furthermore, cations Al^{3+} (0.51A°), Ga^{3+} (0.62A°), Fe^{3+} (0.64A°), Ge^{4+} (0.53A°), Ti^{4+} (0.64°A) and P^{5+} (0.35°A) have also been detected as substitutes.

Ionizing radiation can cause colors in quartz due to the presence of paramagnetic centers and the transformation of non-paramagnetic precursors. The $[AlO_4]$ center (i.e., $[AlO_4/M^+]+e^-$) causes the color in smoky quartz, while the $[FeO_4]$ center (i.e., [FeO4/ M^+].+e^-) causes the purple to pale violet color of amethyst. The artificial smokiness of quartz caused by X-ray and gamma-ray irradiation is the most common. Experiments during quartz synthesis have shown that low growth rates for quartz crystals may favor the incorporation of Al into the quartz lattice giving a high concentration of color centers (Rose *et al.*, 1984).

Bartoll *et al.* (2001) studied ESR study of E_1' center in geological flint. Bennya *et al*. (2002) studied the E_1' center and its role in thermoluminiscence sensitization in quartz. Buscarino and Agnello (2007) studied E' centers from oxygen vacancies in α- SiO_2. Nilges *et al.* (2008, 2009) studied radiation induced defects in quartz single crystal using Electron Paramagnetic Resonance, Electron Nuclear Double Resonance (ENDOR), and Electron Spin Echo Envelop Modulation (ESEEM). Pan and Hu (2009) studied empirical thermal properties of radiation induced defects in quartz. They studied the thermal stabilities and decay kinetics of the peroxy radicals and radiation induced defects in natural quartz from the high grade McArthur river uranium deposit (Athabaska basin Canada). Botis *et al.* (2006, 2008) studied radiation induced defects in drusy quartz minerals which are collected from McArthur river of Athabaska basin of Canada. Sivaramaiah *et al.* (2011) studied the thermal properties of Fe^{3+} center in natural amethyst. Sivaramaiah and Pan (2012) studied the thermal properties of Fe^{3+} center in γ-ray-irradiated natural amethyst. To our best knowledge, there are no previous reports on thermal properties of E_1' in natural and γ-ray-irradiated amethyst. The thermal properties have significant information for knowing the stability, magnetic and exchange interactions. Therefore the author performed original study using EPR spectroscopy.

Sample Preparation and Experimental Procedure

A natural amethyst crystal from the University of Saskatchewan reference mineral collection is selected for this study. This crystal has a dimension of approximately 20 x 10 x 5 cm^3. A Part of the big crystal is cut and pulverized in air in a ceramic mortar for an hour to ensure uniform powder samples for EPR observations. Pentahydrate single crystals of $CuSO_4.5H_2O$, are grounded into powder and used as a standard in the analysis of absolute number of spins. Powders of this sample obtained from pulverization in air are irradiated at room temperature in a ^{60}Co cell with a dose rate of 460 Gy/h for a dose of 10 kGy.

EPR spectra are recorded using a Bruker EMX X-band EPR spectrometer equipped with a high-sensitivity ER 4119 cavity, an automatic frequency controller and an Oxford liquid-helium cryostat at the Saskatchewan Structure Sciences Centre, University of Saskatchewan. An empty amorphous silica tube is first recorded at room temperature to ensure that it is free of any paramagnetic species. This tube is then used for recording powder EPR spectra of the natural amethyst. Powder EPR spectra of the natural amethyst samples, are made in the same tube at room temperature and microwave frequencies of 9.64 GHz. Other experimental conditions included a modulation frequency of 100 kHz, microwave power of 0.02 mW, modulation amplitude of 0.2 mT and spectral resolutions of 0.122-0.273 mT (i.e., 1,024-4,096 field data points over a scan range of 100-500 mT). Powder EPR spectra of the natural amethyst at cryogenic temperatures (90-270 K) were recorded using experimental conditions similar to

those used for the room temperature measurements, except that the microwave frequencies used were at 9.38 GHz. Powder EPR spectra for the $CuSO_4.5H_2O$ standard are recorded with the amethyst sample using the same experimental conditions.

Results

Figs. 1(a) and 1(b) show the EPR spectra of natural amethyst and 10 kGy γ-ray-irradiated natural amethyst. From Fig. 1(a), it is observed that two signals with the effective g values at g ≈4.0 and 2.00 are present in the spectrum. The signals with the effective g values at g = 4.3 and 2.00 are observed from Fig. 1(b). The signals at g≈4, 4.3 are due to Fe^{3+} ions. The weak and sharp signal at g = 2.00 is due to the well established E_1'. Figs. 2(a) and 2(b) show the EPR spectra of natural and 10 kGy gamma-ray-irradiated amethyst observed at 90, 180 and 270 K.

The absolute spins between the Zeeman levels (N) can be calculated from the area under the absorption curve with that of a standard ($CuSO_4.5H_2O$) of known concentration. Weil and Bolton (2007) gave the following formula including the experimental parameters of both the sample and the standard

$$N = \frac{A_x(scan_x)^2\, G_{std}(B_m)_{std}(g_{std})^2\, [S(S+1)]_{std}(N_{std})}{A_{std}\,(scan_{std})^2\, G_x\,(B_m)_x\,(g_x)^2\,[S\,(S+1)]_x} \quad (1)$$

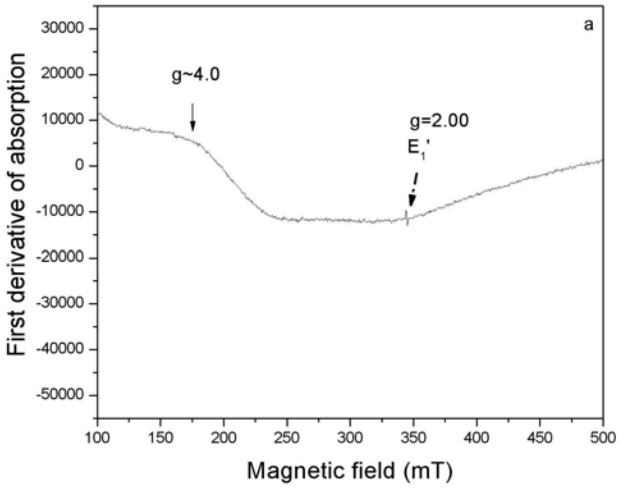

(A)

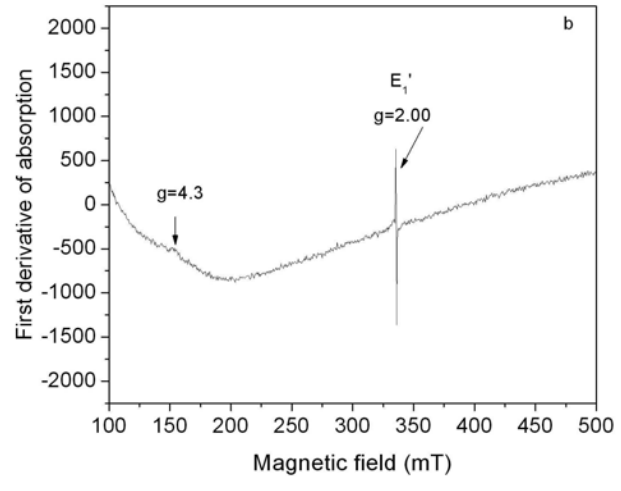

(B)

Fig. 1: EPR spectrum of (A) natural amethyst at 296 K and (B) 10 kGy gamma-ray-irradiated amethyst at 296 K

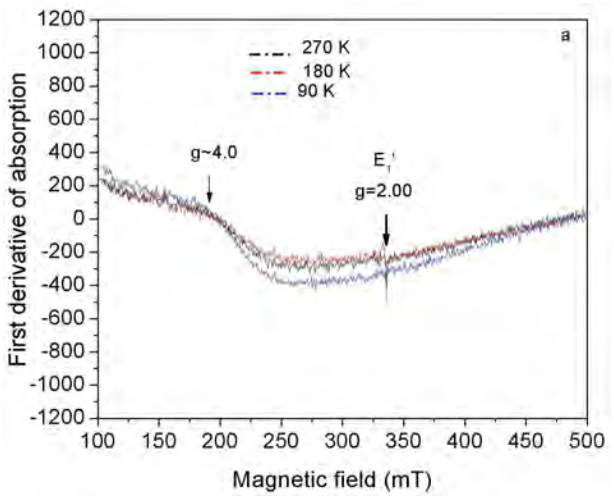

(A)

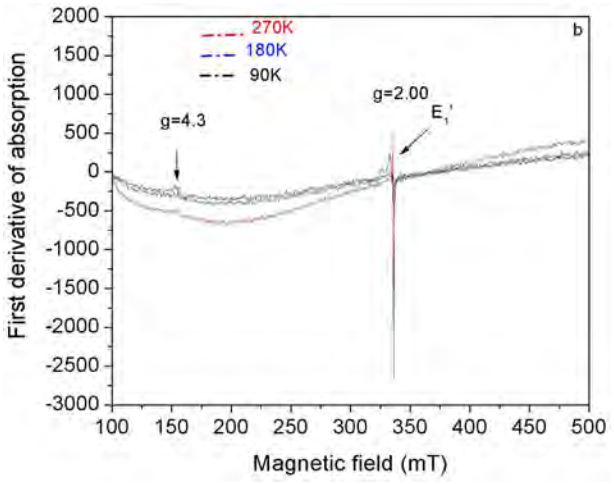

(B)

Fig. 2: EPR spectra of (A) natural amethyst at 270, 180 and 90 K (B) 10 kGy gamma-ray irradiated amethyst at 270, 180 and 90 K

where A is the area under the absorption curve, scan is the magnetic field corresponding to the unit length of the spectrum, G is the amplitude, B_m is the modulation amplitude, g is the g factor, S the spin of the ions in the ground state (S = 1/2 for E_1' and 1/2 for Cu^{2+} ions). The subscripts 'x' and 'std' denote the sample and the standard respectively. N_{std} denotes number of spins in 100 mg of $CuSO_4.5H_2O$ standard. The number of spins of E_1' for natural and 10 kGy γ-ray-irradiated amethyst are determined as 7.58×10^{21} and 0.46×10^{21} per g at room temperature, respectively. Fig. 3 shows the variation of absolute number of spins with temperature variation from 90 to 296 K for E_1' in natural and 10 kGy γ-ray-irradiated amethyst.

The Gibbs free energy can be calculated using the expression (Wigner *et al*., 1930)

$$\Delta G = 2.303\ RT \log_{10} (k_B T/\lambda h), \quad (2)$$

where ΔG is the Gibbs free energy, R is the Universal gas constant, k_B is the Boltzmann constant, T is the absolute temperature, λ is the rate constant and is equal to the number of spins per m^3, h is Planck's constant. The Gibbs energy of the E_1' at g = 2.00 has been found to be –68.49 and –61.61 (kJ/mol) for natural and 10 kGy gamma-ray-irradiated amethyst at room temperature, respectively. The values are consistent with the values reported in literature (Thompson, 1974). Fig. 4 shows the Gibbs free energy variation with temperature variation from 90 K to 296 K for E_1' of natural and 10 kGy gamma-ray-irradiated amethyst. From this figure it is evident that the Gibbs free energy increases with the decrease of temperature from 296 K to 90 K in accordance with the Boltzmann distribution law.

The activation energy can be calculated using the expression (Sivaramaiah *et al*., 2011)

$$\lambda = A\, e^{-E}a^{/RT}, \quad (3)$$

where λ is the rate constant and is equal to number of spins/m^3, A is the pre-exponential coefficient; R is the universal gas constant; T is absolute temperature and E_a is the activation energy. Figs. 5(a) and 5(b) show that $\log_{10}$ (N) of the E_1' center at g = 2.0 for natural and 10 kGy γ-ray-irradiated amethyst correlates linearly with the reciprocal of temperature (1/T). The slope of this correlation yields the activation energy Ea at –0.03 and –0.02 eV, for E_1' of natural and 10 kGy γ-ray-irradiated amethyst, which is consistent with those reported for Fe^{3+} in amethysts (Sivaramaiah *et al*., 2011; Sivaramaiah and Pan, 2012). The pre-exponential coefficient (PEC) has been determined to be 56, 54 per second for E_1' in natural and 10 kGy γ-ray-irradiated amethyst from

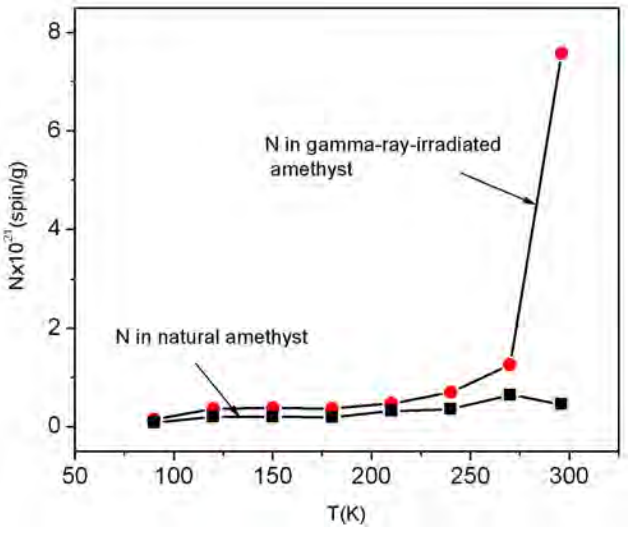

Fig. 3: Absolute number of spins of E_1' in (a) natural amethyst and (b) 10 kGy gamma-ray-irradiated amethyst at different low temperatures (270-90 K)

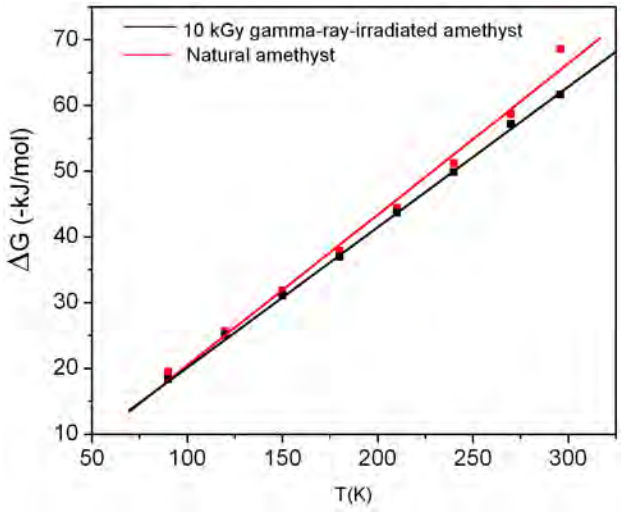

Fig. 4: Gibbs free energy of E_1' in (a) natural amethyst and (b) 10 kGy gamma-ray-irradiated amethyst, at 296 K and different low temperatures (270-90K)

the intercept on Y axis of Figs. 5(a) and 5(b). In the calculation of activation energy, we observed negative slope from origin programme and therefore the activation energy is negative. The slope of $\log_{10}N$ vs 1/T may be positive or negative. If we take the sign and interpret the results, then the information is excellent. With manual calculation, the slope is always positive. The first data point of Fig. 5(a) is not taken for calculations since it is deviating the remaining points.

Figs. 5(a) and 5(b) also show that $\log_{10}$ (N/T) correlates linearly with the reciprocal of temperature

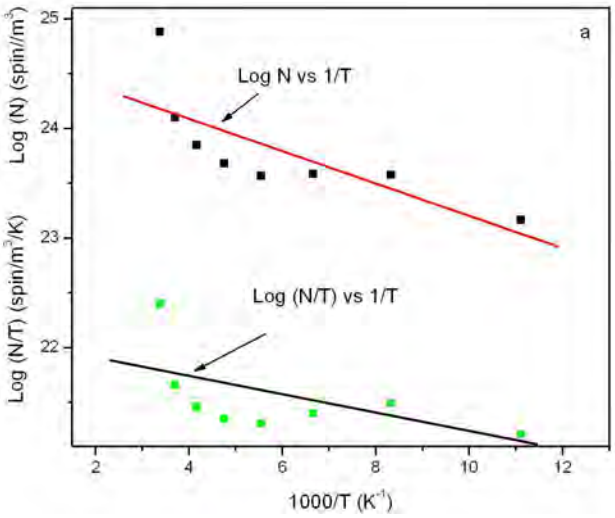

(A)

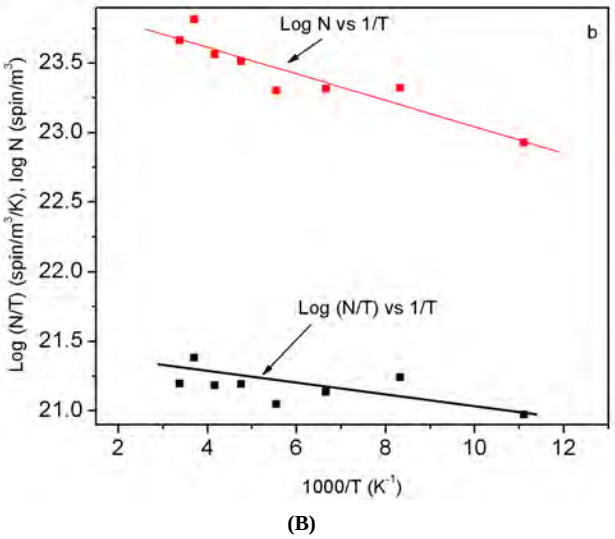

(B)

Fig. 5: LogN versus 1/T , log(N/T) versus (1/T) for E_1' of (a) natural amethyst (b) 10 kGy gamma-ray-irradiated natural amethyst

for E_1' of natural amethyst and 10 kGy gamma-ray-irradiated amethyst. The intercept of this graph gives the entropy ΔS at –0.27, –0.34 meV for E_1' of natural and 10 kGy γ-ray-irradiated amethyst and are comparable with the value reported in literature (Santillan *et al.*, 1972). The slope of this correlation yields the enthalpy ΔH at –0.016 and –0.057 eV and are consistent with the value reported in literature (Hovis, 1988). The slope of $\log_{10}$N/T vs 1/T here also negative from origin programme and hence the enthalpy is negative.

The magnetic susceptibility can be determined using the expression (Dekker, 2006)

$$\chi = \frac{N g^2 \beta^2 S (S+1)}{3k_B T}, \qquad (4)$$

where N is number of spins per m^3, g =2.0, β is Bohr magneton, S is spin angular momentum quantum number, k_B is Boltzmann constant and T is temperature. Since E_1' has S value and no L value and hence the present equation is used. This equation is good for defect centers. The same equation is used for TM ions also. The magnetic susceptibility of E_1' in natural and 10 kGy γ-ray-irradiated amethyst at room temperature is found to be 16.0 x 10^{-2}, 97.36 x 10^{-4} m^3/kg, respectively. Fig. 6 shows the temperature dependence of reciprocal of magnetic susceptibility of E_1' center of natural and 10 kGy γ-ray-irradiated

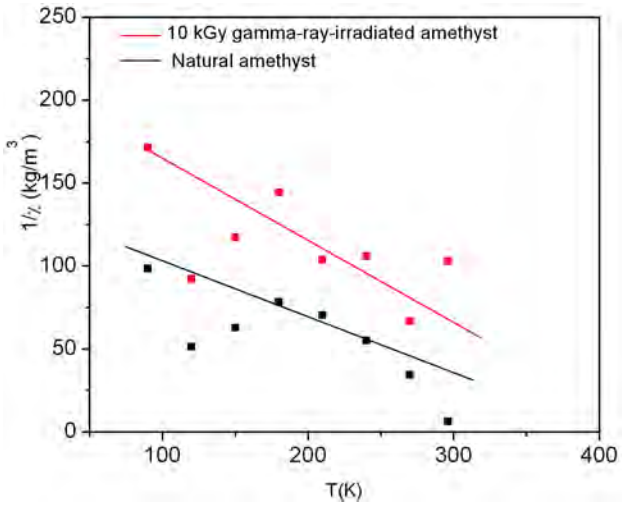

Fig. 6: Reciprocal of magnetic susceptibility and temperature plot of E_1' in natural and gamma-ray-irradiated amethyst

amethyst. The intercept on X-axis of the plot gives Curie temperature and the reciprocal of the plot gives Curie constant. Thus, the values of Curie constant and Curie temperature for E_1' are found to be 423 K and –3.29 emu/mol in natural amethyst. These values for E_1' of 10 kGy γ-ray-irradiated amethyst are found to be 423 K and –3.62 emu/mol. The observed values are precise for defect centers.

The exchange field B_e can be calculated using the expression (Kittel, 1996)

$$B_e = \frac{k_B \theta}{\mu_B}, \quad (5)$$

where k_B is the Boltzmann constant, θ is the Curie temperature and μ_B is the Bohr magneton. The exchange field is also called as internal molecular field and is proportional to the magnetization. The magnitude of the exchange field may be of the order of 1000 T (Kittel, 1996).

The exchange integral J can be calculated using the expression (Dekker, 2006)

$$J = \frac{k_B \theta}{3}, \quad (6)$$

where k_B is Boltzmann constant, θ is the Curie temperature.

The exchange interaction energy can be determined using the expression (Dekker, 2006)

$$E = -2 J \Sigma S_i.S_j. \quad (7)$$

where J is the exchange integral S_i and S_j are the nearest neighbor spins.

Discussion

The sharp signal at g = 2.00 has been attributed to the well known oxygen-vacancy electron center E_1' (Weeks, 1956; Silsbee, 1961; Rudra and Fowler, 1987). The point defects in quartz are classified into two types namely impurity defects and vacancy defects (Carbonaro *et al*., 2006). The vacancy defect involves either a missing oxygen atom or an absent silicon atom. A missing oxygen atom is responsible for the formation of a number of electron like paramagnetic defects including the well known E_1' center. A silicon vacancy in the quartz structure has four dangling bonds all of which could lead to hole trapping and formation of hole like centers. The signals with the effective g values at g = 4.0, 4.3 are attributed to Fe^{3+} ions in orthorhombic symmetry (Hofmeister and Rossman, 1984; Rager and Schneider, 1986).

The number of spins were decreased by 7.12 x 10^{21} with the γ-ray-irradiation. This is due to the decrease of unpaired spins with the γ-ray-irradiation. The Gibbs potential has increased by 6.88 kJ/mol with the γ-ray-irradiation. The negative sign indicates that there is strong attractive interaction between E_1' and the amethyst lattice. Larger the Gibbs free energy, smaller the stability (Sivaramaiah and Lakshmanrao, 2012). Thus stability is greater in natural amethyst than in γ-ray-irradiated amethyst.

The activation energy represents minimum energy required to liberate an electron from E_1' in this amethyst (Sivaramaiah, 2011). The activation energy is slightly more in 10 kGy γ-ray-irradiated amethyst (–0.02 eV)) than natural amethyst (–0.03 eV). Thus the energy required to liberate an electron from amethyst lattice is more in γ-ray-irradiated amethyst than its natural as-is amethyst. The pre-exponential coefficient is slightly more in natural amethyst than in γ-ray-irradiated amethyst. This indicates that the collision frequency between the spins and the quartz lattice is more in natural amethyst than the γ-ray-irradiated amethyst.

The enthalpy (–0.016 eV) is more in natural amethyst than the γ-ray-irradiated amethyst (–0.057 eV). The entropy ΔS is comparable in both the amethysts. The negative sign indicates that more order is present and less disorder is present in both the amethysts. These values of ΔS and ΔH indicate strain and exchange interaction at the domain boundaries of amethyst.

The entropy and enthalpy of activation represent total heat content in minerals. These parameters are useful for measuring the thermal conductivity of minerals. They also represent strain and exchange

Table 1: Absolute spins (N), Gibbs free energy (ΔG), magnetic susceptibility (χ), exchange field (Be), exchange integral (J), exchange interaction energy (E) and line-width ΔBpp of E_1' in natural and γ-ray-irradiated amethyst

	N (spin/g)	ΔG (kJ/mol)	χ(m^3/kg)	Be (T)	J (eV)	E (eV)	ΔBpp (mT)
Natural amethyst	$7.58x10^{21}$	–68.49	$16.0x10^{-2}$	630	0.012	–6.1	1.15
Gamma-ray -irradiated amethyst	$0.46\ x10^{21}$	–61.61	$97.36x10^{-4}$	630	0.012	–6.1	0.8

interaction at the field boundaries of the domains in minerals (Sivaramiah and Pan, 2012). The decrease of both ΔH and ΔS with irradiation is due to decrease of the density of mobile/conduction electrons. The pre-exponential coefficient is useful for exploring the information on spin density, spin orientation and spin concentration. The high Curie temperature (423 K) of E_1' in both the amethysts suggests that ferromagnetic interactions are dominant in both the amethysts. Such type of high Curie temperature value is expected for defects such as E_1'. The negative Curie constant indicates that strong antiferrmagnetic interactions are found in both the amethysts. Such type of dual magnetic interactions is expected in amethysts.

The exchange field Be is found to be 630 T for E_1' of 10 kGy γ-ray-irradiated amethyst and as-is amethyst. The exchange integral is found to be 0.0122 eV for E_1' of γ-ray-irradiated and natural amethyst. The exchange interaction energy is found to be –6.1 meV for E_1' of both the amethysts. The negative sign indicates there is strong attractive interaction between the spins of E_1' and amethyst lattice in both the amethysts. The exchange field Be, exchange integral J and exchange interaction energy E are equal for E_1' in γ-ray-irradiated amethyst and as-is amethyst.

The exchange integral J explains the nature of magnetic state and the stability of magnetic state. If the exchange integral is positive, the magnetic state is stable. If the exchange integral is negative, the magnetic state is unstable (Dekker, 2006).The exchange integral in the present case is positive and supports for the stability of the magnetic system. The exchange energy appears in the total energy as if there exists a direct coupling between the two spins. It must be emphasized, however, that the exchange interaction is fundamentally electrostatic and that the spin enters into the energy expression as a consequence of the Pauli Exclusion Principle (Dekker, 2006). The line-width for E_1' of natural amethyst is found to be 1.15 mT and its value for 10 kGy γ-ray-irradiated amethyst is found to be 0.8 mT. Tabel 1 shows absolute spins (N), Gibbs free energy (ΔG), magnetic susceptibility (χ), exchange field (Be), exchange integral (J), exchange interaction energy (E) and line-width ΔBpp of E_1' in natural and gamma-ray-irradiated amethyst.

Conclusions

The Gibbs free energy of E_1' in both the amethysts is found to dependant on temperature. From the entropy value of E_1' in both the amethysts, it is observed that more order and less disorder is present. The exchange field, exchange integral and exchange interaction energy are found to be equal for E_1' of both the amethysts.

Acknowledgements

The author is thankful to Prof. Y. Pan for helpful discussions. The author is also thankdul to the Editor of INSA for incisive criticism for betterment of the manuscript.

References

Agnello S, Boscaino R, Buscarino G, Cannas M and Gelardi F M (2002) *Phys Rev B* **66** 113-201

Bartoll J, Schwarcz H P and Rink W J (2001) *Radiat Meas* **33**

893-898

Bennya P G, Gundu Raob T K and Bhatt B C (2002) *Radiat Meas* **35** 369-373

Botis S M, Pan Y, Bonli T, Xu Y, Zhang A, Nokhrin S and Spuck V (2006) *Can Mineral* **44** 1387-1402

Botis S M, Pan Y, Nokhrin S and Nilges M J (2008) *Can Mineral* **46** 125-138

Buscarino G and Agnello S (2007) *J Non-Cryst Solids* **353** 577-580

Carbonaro C M, Fio renti ni V and Berardini F (2001) *Phys Rev Lett* **86** 3064-3067

Dekker A J (2006) Solid State Physics, Department of Electrical Engineering, University of Groningen, Netherlands

Hofmeister A M and Rossman G R (1984) *Phys Chem Miner* **11** 213-224

Hovis G L (1988) *J Petrol* **29(4)** 731-763

Kittel C (1996) Introduction to Solid State Physics, seventh edition, John Wiley & Sons, Inc., New York

Nilges M J, Pan Y and Mashkovtsev R I (2008) *Phys Chem Miner* **35** 103-115

Nilges M J, Pan Y and Mashkovtsev R I (2009) *Phys Chem Miner* **36** 61-73

Pan Y and Hu B (2009) *Phys Chem Minerals* DOI 10.1007/s00269-009-0288-0

Rager H and Schneider H (1986) *Am Mineral* **71** 105-110

Rocha F D G, Oliveria M L, Cecatti S G P and Caldas L V E (2003) *Appl Radiat Isot* **58** 85-88

Rose T P, Rossman R E and Criss G R (1984) *Chem Geol* **114** 185-189

Rudra J K and Fowler W B (1987) *Phys Rev B* **35** 8223-8230

Rudra J K, Fowler W B and Feigl F J (1985) *Phys Rev Lett* **55** 2614-2617

Santillan-Medrano J M and Bohn Hinrich L (1972) *Soil Sci Soc Am J* **36** 835-838

Santos A J J, de Lima J F and Valerio M E G (2001) *Radiat Meas* **33** 427-430

Sawakuchi G O and Okuno E (2004) Instrum Nucl *Methods Phys Res* B **218** 217-221

Schilles T, Poolton N R J, Bulur E, BZtter-Jensen L, Murray A S, Smith G M, Riedi P C and Wagner G A (2001) *J Phys D* **34** 722-731

Silsbee R H (1961) *J Appl Phys* **32** 1459-1462

Siva Ramaiah G and Lakshmana Rao (2012) *J Spectrochimica Acta Part A: Molecular and Biomolecular Spectroscopy* **98** 105-109

SivaRamaiah G and Pan Y (2012) *Phys Chem Minerals* **39** 515-523

SivaRamaiah G, Lin J and Pan Y (2011) *Phys Chem Minerals* **38** 159-167

Thompson A B (1974) *Contrib. Mineral Petrol* **48** 123-136

Wang A, Haskin L A and Cortez E (1998) *Appl Spectrosc* **52** 477-487

Weeks R A and Nelson C M, (1960) *J Am Ceram Soc* **43** 399-404

Weeks R A, Magruder R H and Stesmans, Andre' (2008) *J Non-Cryst Solids* **354** 208-216

Weeks R A (1956) *J Appl Phys* **27** 1376-1381

Weil J A and Bolton J R (2007) Electron Paramagnetic Resonance: elementary theory and practical applications. Wiley, New York

Wigner, Eyring, Polanyi and Evans (1930) Transition state theory of chemical reactions.